Li-intercalated TiS_2 Nanotubes

Lithium Intercalation in Open-Ended TiS_2 Nanotubes**

Jun Chen, Zhan-Liang Tao, and Suo-Long Li*

There has been considerable recent interest in the synthesis and characterization of transition-metal disulfide nanotubes. The significant breakthrough in obtaining WS_2 and MoS_2

[*] Prof. Dr. J. Chen, Dr. Z.-L. Tao, Dr. S.-L. Li
Institute of New Energy Materials Chemistry
Nankai University, Tianjin 300071 (P.R.China)
Fax: (+86) 22-2350-9118
E-mail: chenabc@nankai.edu.cn

[**] The authors acknowledge support from the Trans-Century Distinguished Talent Project (Grant No. 200248) and the Scientific Research Foundation for the Returned Overseas Chinese Scholars (Grant No. 2002247; State Education Ministry). We are also thankful to Professors C. X. Cui and X. Q. Zhu, and Drs. Y. T. Shen and Q. Xu for their experimental assistance.

 DOI: 10.1002/ange.200250573

nanotubes by Tenne and co-workers[1,2] was accomplished through either the hydrosulfurization of a very thin film of tungsten or the gas–solid reaction between MO_3 (M = W, Mo) and H_2S in a reducing atmosphere at elevated temperatures (800–1000 °C). Methods, such as chemical transport,[3] solution routes,[4] in situ heating,[5] activation techniques,[6] and gas–solid reactions[7,8] can all be used to prepare MS_2 nanotubes. Recently, Remskar et al.[9] synthesized bundles of very long single-walled MoS_2 nanotubes (9.6 Å in diameter) using a C_{60}-catalyzed transport reaction. Furthermore, Nath and Rao[10,11] successfully prepared multiwalled transition-metal disulfide nanotubes of groups 4 and 5 through the thermal decomposition of metal trisulfides in a hydrogen atmosphere at 800–1000 °C. However, in comparison with their HfS_2 and ZrS_2 counterparts, TiS_2 nanotubes are more sensitive to electron beams,[11] and details of their characterization were not made available.

Layered transition-metal dichalcogenides MS_2 (such as TiS_2 and MoS_2) are of great interest as they act as host lattices by reacting with a variety of guest atoms or molecules to yield intercalation compounds, in which the guest is inserted between the host layers.[12] In layered MS_2 materials, atoms within a layer are bound by strong covalent forces, while the individual layers are held together by van der Waals (vdW) interactions. The weak interlayer vdW interactions allow foreign atoms or molecules to be introduced between the layers through intercalation.[13] Zak and co-workers[14] have accomplished the intercalation of alkali metals into fullerene-like MS_2 (M = W, Mo) nanoparticles, and have investigated the properties of these intercalation compounds. Their results show that the inert vdW surface of the closed nanoparticles presents a diffusion barrier for the intercalation process. Since the MS_2 nanotubes are formed through the folding of layered nanoparticles, it may be imagined that hollow multiwalled nanotubes with open-ended tips are suitable materials for atomic or molecular intercalation. Here, we report the low-temperature synthesis of open-ended TiS_2 nanotubes, and the subsequent intercalation of lithium into the nanotube by a solution-based chemical approach.

TiS_2 nanotubes were prepared by the following procedures: $Na_2S{\cdot}9H_2O$ (> 99 % purity, Aldrich) was dried under vacuum (~ 10^{-5} bar) at 200 °C for 24 h over P_2O_5 to remove the water of crystallization. THF was refluxed for 6 h in the presence of $LiAlH_4{\cdot}8$THF and subsequently distilled under argon. Only water-free Na_2S and THF were used in the subsequent reactions. A solution of $TiCl_4$ (3.8 g, 20 mmol, Aldrich) in THF (150 mL) was prepared in a glove box filled with pure argon (99.999 %) in the presence of an oxygen scavenger and a sodium drying agent. At 40 °C, crystalline Na_2S (3.1 g, 40 mmol) was added to the above solution while stirring. The mixture was then cooled after 30 min. The dark-brown solid was filtered, and washed with THF and methanol several times to remove NaCl formed during the reaction. The powder was then transferred into a teflon-lined stainless-steel tube, which was flushed with H_2 and maintained at 200 °C for 6 h to obtain pure TiS_2 nanotubes while removing the solvent. In a typical synthesis, about 2 g of the product was recovered. The process employed to obtain the TiS_2 nanotubes can be described thus:

$$TiCl_4 + 2\,Na_2S \xrightarrow{40\,^{\circ}C,\ THF} TiS_2 + 4\,NaCl \quad (1)$$

$$TiS_2\ (\text{nano/amorphous particles}) \xrightarrow[H_2]{200\,^{\circ}C} TiS_2\ (\text{nanotubes}) \quad (2)$$

The change in standard Gibbs free energy ($\Delta G°$) of reaction (1) is about $-431.5\ kJ\,mol^{-1}$, which implies that the reaction strongly favors the formation of TiS_2.

The as-prepared samples were characterized by scanning electron microscopy (SEM; JEOL JSM-5600 microscope), transmission electron microscopy (TEM; Philips Tacnai F20 microscope, 200 kV), energy-dispersive X-ray spectroscopy (EDXS), powder X-ray diffraction (XRD; Rigaku INT-2000 X-ray generator, $Cu_{K\alpha}$ radiation), X-ray photoelectron spectroscopy (XPS; Shimadzu Electron ESCA-3400 spectroscope, $Mg_{K\alpha}$ radiation), and Brunauer–Emmett–Teller (BET) nitrogen sorption (Shimadzu-Micromeritics ASAP 2010 Instrument).

Characterization of the as-prepared samples suggested that the low-temperature synthesis was successful in preparing open-ended nanotubes. Figure 1 shows a characteristic SEM image of the as-prepared products. It can be seen that a large number of nanotube filaments are distributed homogeneously over a wide area, and that they are a number of micrometers in length and several tens of nanometers in diameter. A significant proportion (> 95 %) of the sample exhibits a tubular structure.

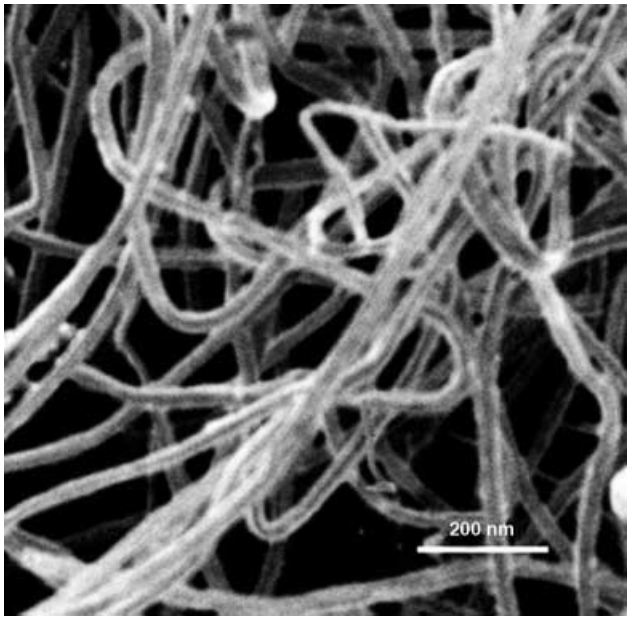

Figure 1. SEM image of the as-prepared TiS_2 nanotubes.

This low-temperature method also gave a satisfactory yield of multiwalled TiS_2 nanotubes with open-ended tips, as can be observed from TEM and high-resolution TEM (HRTEM) analyses (Figure 2). A low-magnification TEM image of a typical TiS_2 sample is shown in Figure 2a, from which it can be seen that the sample consists of single nanotubes and nanotube bundles. Both the single nanotubes and the nanotube bundles exhibit uniform tubular structures

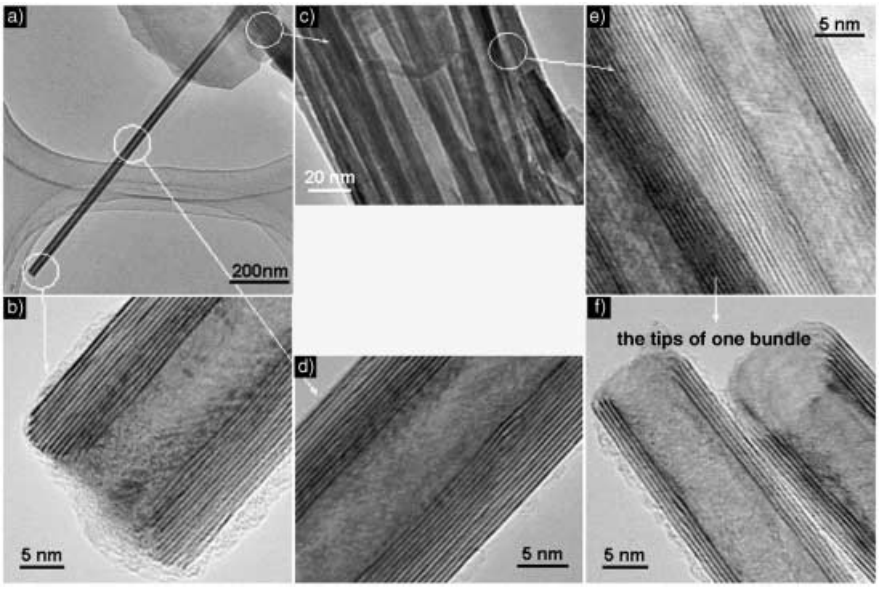

Figure 2. Representative low-magnification (a, c) and high-resolution (b, d, e, f) TEM images of multiwalled TiS_2 nanotubes.

with a length of approximately 2 μm, an outer diameter of approximately 30 nm, an inner diameter of approximately 10 nm, and an interlayer spacing of approximately 0.57 nm (Figure 2b, d, e, and f). Note that the nanotube tips are open and that there is little evidence for the coexistence of an amorphous phase at the tube tips (Figure 2b and f).

The chemical composition of both the individual nanotubes and the bundles was analyzed by EDXS, and both were shown to have a Ti/S atomic ratio of 1:2. XPS analysis demonstrates that the valence of the Ti centers within the nanotubes is +4, and the peak is assigned to Ti $2p_{3/2}$ orbital in TiS_2, which is characterized by a detected binding energy of 458 eV in a well-defined spin-coupled curve. Powder XRD analysis of the product confirmed that the sample was composed of the 1T-TiS_2 phase in high purity, with hexagonal lattice parameters ($a = b = 3.405$, $c = 5.697$ Å) that are in good agreement with those of polycrystalline TiS_2 ($a = b = 3.4049$, $c = 5.6912$ Å; ICDD–JCPDS card No. 15-0853). The c value from the XRD pattern is also consistent with the interlayer spacing observed from the HRTEM images shown in Figure 2. Thus, the EDXS, XPS, and XRD measurements have unambiguously demonstrated that the tubular structures in our sample are multiwalled TiS_2 nanotubes with open-ended tips.

Since multiwalled nanotubes with open-ended tips potentially have a lower diffusion barrier for the intercalation process than their closed counterparts, the introduction of lithium into the layers of the nanotubes was attempted by a solution-based approach. Lithium intercalation into TiS_2 nanotubes can be described thus:

$$TiS_2 + x\,Li^+ + x\,e^- \rightarrow Li_xTiS_2$$

Li_xTiS_2 samples ($x = 0.12$, 0.52, and 1.0) were prepared by the chemical intercalation of TiS_2 nanotubes using *n*BuLi (1.6 M, Aldrich) as the Li source.[15] The nanotubes were suspended in hexane, and *n*BuLi was added while stirring the reaction mixture. After 24 h of vigorous stirring, the samples were filtered, washed with THF, and dried in Ar at 40 °C for 5 h. The Li/Ti ratio was determined by chemical inductively coupled plasma (ICP) spectroscopy. The surface area of the $LiTiS_2$ and TiS_2 nanotubes was 32 and 25 $m^2 g^{-1}$, respectively, as determined by BET N_2 adsorption–desorption isotherms. All procedures for handling the materials (BET Bell tube, XRD and TEM specimen holders) were carried out in a glove box filled with pure Ar in order to prevent the reaction of Li with air. For XRD measurements, the Li_xTiS_2 nanotubes were coated with paraffin oil, smeared on a glass substrate, and then covered by an adhesive tape to prevent the sample from reacting with oxygen and/or moisture during the measuring process.[16] For TEM observations, the sample grid and specimen holder were prepared in the glove box and transferred to a glove bag (Cheltenham, Model X-27–27H). During the transfer of the specimen holder to the TEM chamber, special care was taken to minimize the exposure of the sample grid to the atmosphere.

XRD of the lithium-intercalated samples indicates that the nanotube structure of TiS_2 is maintained after intercalation. Figure 3a shows XRD patterns for the TiS_2 nanotubes before lithium intercalation, and for the resulting Li_xTiS_2 products. Upon intercalation, the (001) peak shifts to lower angles, which indicates an expansion of the interlayer spacing. Figure 3b shows the lattice parameters a and c obtained from the XRD for samples with different x values. It can be seen that only very slight differences were observed in the value of the lattice constant a, while the lattice spacing c is strongly correlated to the intercalated lithium quantity x. The largest interlayer spacing (6.3 Å) was observed when $x = 1$, which corresponds to an expansion in the c axis of approximately 10.5%. It has been previously reported that lithium intercalation in polycrystalline TiS_2 leads to a single homogeneous phase with a lattice expansion of approximately 10% for the entire intercalation range, up to $x = 1$ in Li_xTiS_2.[17] Therefore, lithium intercalation in the open-ended TiS_2 nanotubes was as effective as that of their polycrystalline counterparts.

The morphology of the lithium-intercalated TiS_2 nanotubes was further investigated by HRTEM. Figure 4 shows such images recorded for the $LiTiS_2$ sample. It was found that individual intercalated nanotubes were evenly aligned and distributed (Figure 4a). The observed interlayer spacing is about 6.3 Å, which is consistent with the XRD data shown in Figure 3. The lithium-intercalated TiS_2 nanotubes are somewhat sensitive to electron-beam irradiation during HRTEM investigations. This is believed to result from lithium being

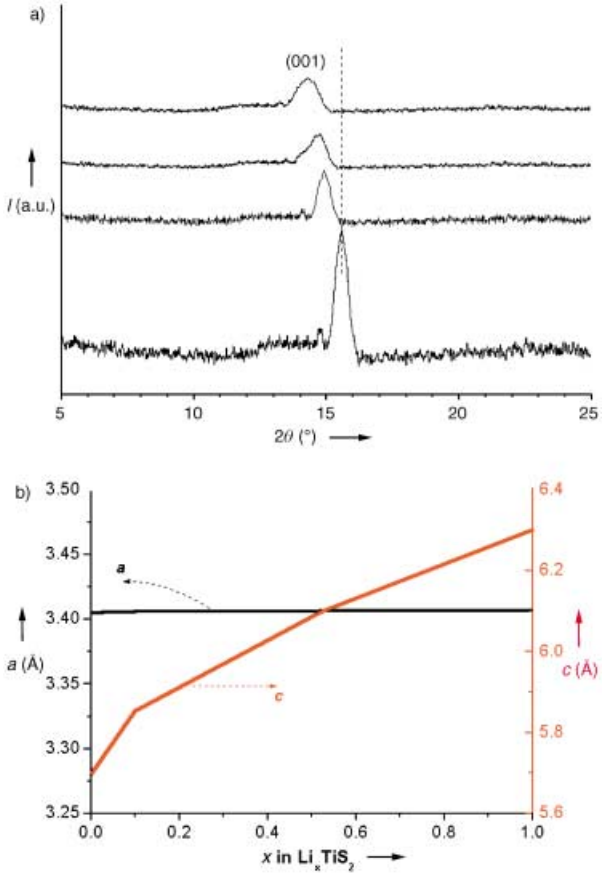

Figure 3. a) XRD patterns of lithium-intercalated Li_xTiS_2 nanotubes (bottom to top: $x = 0$, 0.12, 0.52, and 1.0, respectively); b) lattice parameters *a* and *c* of Li_xTiS_2 nanotubes.

"pumped out" from the nanotubes upon irradiation, which is consistent with qualitative analysis that shows a decrease in the interlayer spacing for the intercalated TiS_2 nanotubes after relatively long irradiation periods (Figure 4c and d). After irradiation for 5 s, the interlayer spacing of the nanotubes is about 6.3 Å (Figure 4b), while after 40 and 60 s of intensive electron-beam irradiation, the interlayer spacing of the nanotubes decreases to approximately 6.1 (Figure 4c) and 6.0 Å (Figure 4d), respectively.

It should be emphasized that some of the walls of the intercalated TiS_2 nanotubes were transformed to an amorphous phase and that more defects were observed after further subjection to intense beam irradiation (Figure 4e). The inset in Figure 4e shows the electron diffraction pattern, which exhibits a hexagonal arrangement of the remaining layers and indicates the axis of the tube is the perpendicular to the *c* axis. In addition, the halo pattern in the electron diffraction pattern reveals the strong incoherent scattering of the electron beam caused by the amorphous phase of TiS_2 around the tube walls. Since this beam sensitivity makes the electron-diffraction analysis difficult, further HRTEM and EDXS measurements were not carried out. Nonetheless, the present XRD and HRTEM observations confirm that the increase in basal spacing can be attributed to the intercalation of lithium. As is already known, the octahedral and tetrahedral interstitial sites in crystalline TiS_2 are available for the intercalation of lithium. In general, the octahedral sites are energetically more favored,[13,18] which leads to a possible maximum intercalation level of one lithium atom per formula unit. The intercalation of lithium within the vdW spacings results in the expansion of the host structure along the *c* axis.

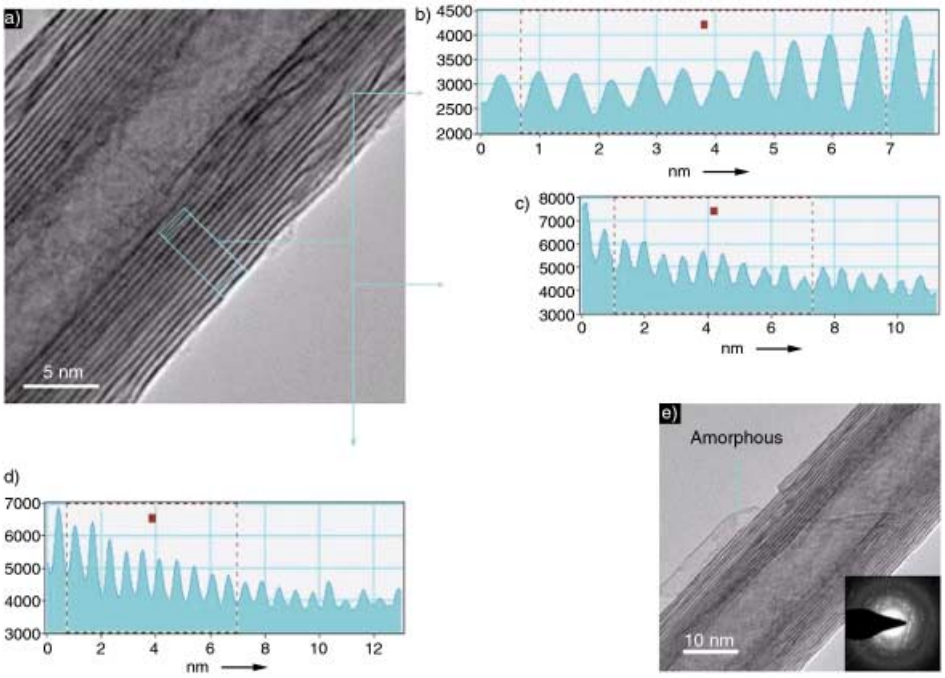

Figure 4. a) HRTEM image of an individual $LiTiS_2$ nanotube and charts of the interlayer spacing of the nanotubes after electron-beam irradiation of 5 (b), 40 (c), and 60 s (d) duration; e) HRTEM image of the $LiTiS_2$ nanotube shown in (a) after irradiation for 60 s (inset: the corresponding electron diffraction pattern).

In conclusion, multiwalled TiS_2 nanotubes with open-ended tips have been successfully synthesized through a low-temperature solution route. It is believed that this rational route can be extended for the synthesis of other similar nanotubes, by starting from the layered structures in solution. Moreover, it can be shown that such TiS_2 nanotubes are very effective toward lithium intercalation while maintaining a homogeneous phase, despite their extreme sensitivity to electron-beam damage. Current work is directed towards further study of the intercalation–deintercalation of alkali metals, hydrogen, and organic molecules in TiS_2 nanotubes. In principle, such intercalated nanotubes should allow elucidation of the mechanism of superlattice formation, high-energy storage systems, and nanophase catalytic reactions.

Received: November 18, 2002 [Z50573]

Keywords: intercalations · lithium · nanotubes · sulfides · titanium

[1] a) R. Tenne, L. Margulis, M. Genut, G. Hodes, *Nature* **1992**, *360*, 444; b) L. Margulis, G. Salitra, R. Tenne, *Nature* **1993**, *365*, 113; c) M. Hershfinkel, L. A. Gheber, V. Volterra, J. L. Hutchison, L. Margulis, R. Tenne, *J. Am. Chem. Soc.* **1994**, *116*, 1914; d) Y. Feldman, E. Wasserman, D. J. Srolovitz, R. Tenne, *Science* **1995**, *267*, 222.

[2] a) R. Tenne, *Adv. Mater.* **1995**, *7*, 965; b) M. Homyonfer, B. Alperson, Y. Rosenberg, L. Sapir, S. R. Cohen, G. Hodes, R. Tenne, *J. Am. Chem. Soc.* **1997**, *119*, 2693; c) R. Tenne, M. Homyonfer, Y. Feldman, *Chem. Mater.* **1998**, *11*, 3225; d) A. Rothschild, R. Popovitz-Biro, O. Lourie, R. Tenne, *J. Phys. Chem. B* **2000**, *104*, 8976.

[3] a) M. Remskar, Z. Skraba, M. Regula, C. Ballif, R. Sanjines, F. Lévy, *Adv. Mater.* **1998**, *10*, 246; b) M. Remskar, Z. Skraba, R. Sanjinés, F. Lévy, *Appl. Phys. Lett.* **1999**, *74*, 3633.

[4] a) C. M. Zelenski, P. K. Dorhout, *J. Am. Chem. Soc.* **1998**, *120*, 734; b) H. W. Liao, Y. F. Wang, S. Y. Zhang, Y. T. Qian, *Chem. Mater.* **2001**, *13*, 6; c) Y. D. Li, X. L. Li, R. L. He, J. Zhu, Z. X. Deng, *J. Am. Chem. Soc.* **2002**, *124*, 1411.

[5] a) Y. Q. Zhu, W. K. Hsu, N. Grobert, B. H. Chang, M. Terrones, H. Terrones, H. W. Kroto, D. R. M. Walton, *Chem. Mater.* **2000**, *12*, 1190; b) W. K. Hsu, Y. Q. Zhu, C. B. Boothroyd, I. Kinloch, S. Trasobares, H. Terrones, N. Grobert, M. Terrones, R. Escudero, G. Z. Chen, C. Colliex, A. H. Windle, D. J. Fray, H. W. Kroto, D. R. M. Walton, *Chem. Mater.* **2000**, *12*, 3541.

[6] a) M. José-Yacamán, H. López, P. Santiago, D. H. Galván, I. L. Garzón, A. Reyes, *Appl. Phys. Lett.* **1996**, *69*, 1065; b) E. B. Mackie, D. H. Galván, E. Adem, S. Talapatra, G. L. Yang, A. D. Migone, *Adv. Mater.* **2000**, *12*, 495.

[7] M. Nath, A. Govindaraj, C. N. R. Rao, *Adv. Mater.* **2001**, *13*, 283.

[8] a) J. Chen, N. Kuriyama, H. T. Yuan, H. T. Takeshita, T. Sakai, *J. Am. Chem. Soc.* **2001**, *123*, 11813; b) J. Chen, S. L. Li, Q. Xu, K. Tanaka, *Chem. Commun.* **2002**, 1722.

[9] M. Remskar, A. Mrzel, Z. Skraba, A. Jesih, M. Ceh, J. Demsar, P. Stadelmann, F. Lévy, D. Mihailovic, *Science* **2001**, *292*, 479.

[10] M. Nath, C. N. R. Rao, *J. Am. Chem. Soc.* **2001**, *123*, 4841.

[11] M. Nath, C. N. R. Rao, *Angew. Chem.* **2002**, *114*, 3601; *Angew. Chem. Int. Ed.* **2002**, *41*, 3451.

[12] a) M. S. Whittingham, *Prog. Solid State Chem.* **1978**, *12*, 1; b) M. M. Thackeray, J. O. Thomas, M. S. Whittingham, *MRS Bull.* **2000**, *25(3)*, 39.

[13] M. Winter, J. O. Besenhard, M. E. Spahr, P. Novák, *Adv. Mater.* **1998**, *10*, 725.

[14] A. Zak, Y. Feldman, V. Lyakhovitskaya, G. Leitus, R. Popovitz-Biro, E. Wachtel, H. Cohen, S. Reich, R. Tenne, *J. Am. Chem. Soc.* **2002**, *124*, 4747.

[15] W. M. R. Divigalpitiya, R. F. Frindt, S. R. Morrison, *Science* **1989**, *246*, 369.

[16] a) W. Bronger, G. Auffermann, *Angew. Chem.* **1994**, *106*, 1144; *Angew. Chem. Int. Ed. Engl.* **1994**, *33*, 1112; b) M. Olofsson-Mårtensson, M. Kritikos, D. Noréus, *J. Am. Chem. Soc.* **1999**, *121*, 10908; c) J. Chen, N. Kuriyama, Q. Xu, H. T. Takeshita, T. Sakai, *J. Phys. Chem. B* **2002**, *105*, 11214.

[17] M. S. Whittingham, *Science* **1976**, *192*, 1126.

[18] B. van Laar, D. V. W. Ijdo, *Solid State Commun.* **1974**, *3*, 590.

